Shape functions associated with the inverse element formulations

S Faroughi and **H Ahmadian***
School of Mechanical Engineering, Iran University of Science and Technology, Narmak, Tehran, Iran

Abstract: Super-convergent element formulations in local co-ordinates are obtained using inverse strategies. In the inverse approach discretization errors of the element formulation are minimized leading to super-convergent solutions. In the development of the inverse element model, no shape functions are introduced and therefore the task of element transformation from local to global co-ordinates system remains a challenge. In this paper, a procedure is proposed to produce shape functions associated with the inverse element formulations via hierarchical polynomials. A membrane element formulation is developed using inverse strategy as an example and its associated shape functions are determined using hierarchical polynomials. Numerical results indicate higher accuracy of the developed model in global co-ordinates compared to the reported models in the literature for the same element.

Keywords: inverse method, discretization error, shape functions, membrane element

1 INTRODUCTION

In the finite-element method, many admissible shape functions are considered for an element, each resulting in different formulation. The difference among these models is in their accuracy and rate of convergence. There are different approaches to improve accuracy and rate of convergence in finite-element models such as employing the p-element method [1–4], differential equation finite-element method [5–7], non-conforming element [8], etc. An alternative is to adopt an inverse strategy and derive the optimum element formulation in the local co-ordinate system by minimization of the discretization errors in a parametric element model. Discretization errors are those associated with replacing the continuous media by one composed of finite elements. The optimum element formulation is referred to as a formulation that leads to results with super-convergent properties. The inverse method in finite-element formulation was used by Stavrinidis *et al.* [9], who determined discretization errors of rod and beam elements as a function of their characteristic lengths. As the element

characteristic length approaches zero, the discretization errors vanish. Stavrinidis *et al.* [9] obtained new formulations for beam and rod elements by minimizing the discretization errors. Later, Ahmadian *et al.* [10] developed mass and stiffness matrices of a rectangular plate element by minimizing the plate element model discretization errors. Kim [11], Hansson [12], and more recently Fried *et al.* [13, 14] obtained super-convergent element models by eigenvalue convergence analysis for rod, beam, and membrane elements in a local co-ordinate.

These rod, beam, membrane, and bending plate element models obtained using the inverse method [9–14] present the best formulation in the local co-ordinate system, but as no associated shape functions are defined for the element models, they cannot be transformed into global co-ordinates. This deficiency prevents their use in practical problems where the geometry of elements differs from local to global co-ordinates.

This article introduces a method to determine the shape functions associated with optimum element formulation obtained using an inverse method. In the proposed method, hierarchal polynomials are employed to establish the shape functions of super-convergent models. Using the established shape functions, an inverse element formulation can be mapped from local to global co-ordinates systems.

**Corresponding author: School of Mechanical Engineering, Iran University of Science and Technology, Narmak, Tehran, Iran. email: ahmadian@iust.ac.ir*

The hierarchal polynomials have been used as shape functions of transverse vibrating membrane [15] and plate [16–18] elements. In the present research work, the same polynomials are employed to establish the shape functions associated with the super-convergent element models. The coefficients of adopted hierarchal polynomial series are assigned such that the corresponding shape functions satisfy the general requirements of compatibility, completeness, and geometrical considerations and regenerate the super-convergent element formulation.

The rest of the article runs as follows. In section 2, the physical requirements of an element model are discussed. These physical requirements are used to develop a parametric model for the element, and the parameters are assigned by minimizing the model discretization errors. The shape functions associated with these inverse element models is reconstructed using the hierarchal polynomial series as proposed in section 3. The proposed strategy is demonstrated using a simple membrane element with transverse degrees of freedom in section 4. Admissible parametric stiffness matrices for rectangular membrane elements are developed in this section and the unknown parameters are defined by minimizing the discretization error in the element formulation. Subsequently, in this section using hierarchal polynomials, shape functions related to the super-convergent stiffness (SCS) model of the membrane element in transverse motion are produced. Section 5 investigates the convergence rates of the obtained stiffness formulations in local and global co-ordinate systems, followed by the concluding remarks in section 6.

2 PHYSICAL REQUIREMENTS OF AN ELEMENT MODEL

In general, an element model must meet certain requirements. Consider an element with d degrees of freedom and r rigid-body modes. The stiffness matrix $\mathbf{K}$ is symmetric positive semi-definite and of rank d and the rigid-body modes of the element, ϕ_{Ri}, $i = 1, 2, \ldots, r$, form its null space

$$\mathbf{K} \cdot \Phi_{R} = 0, \quad \Phi_{R} = [\phi_{R1}, \phi_{R2}, \ldots, \phi_{Rr}] \tag{1}$$

Also, mass matrix $\mathbf{M}$ is symmetric positive definite and of rank d. If the rigid-body modes are defined on the principal co-ordinates of the element then

$$\Phi_{R}^{T} \mathbf{M} \Phi_{R} = \mathrm{diag}(m, m, m, I_{xx}, I_{yy}, I_{zz}) \tag{2}$$

where m is the element mass and I_{xx}, I_{yy}, and I_{zz} are the moments of inertia. Moreover, if some strain modes of the element such as constant strain modes $\Phi_{C} = [\phi_{c1}, \phi_{c2}, \ldots, \phi_{cn}]$ are known, then further constraints

can be imposed on the stiffness matrix

$$\mathbf{K} \cdot \phi_{ci} = \lambda_{i} \phi_{ci}, \quad i = 1, 2, \ldots, n \tag{3}$$

where λ_{i} corresponds to the strain energy stored in the element at the ith constant strain mode and is defined using the known strain and stress, σ_{i}, distributions

$$\lambda_{i} = \frac{1}{2} \int_{v} \varepsilon_{i} \sigma_{i} \mathrm{d}v \tag{4}$$

The orthogonality relations for the set of rigid-body modes and strain modes are

$$[\Phi_{R} \quad \Phi_{C}]^{T} \mathbf{K} [\Phi_{R} \quad \Phi_{C}] = \begin{bmatrix} 0 & 0 \\ 0 & \Lambda \end{bmatrix},$$

$$\Lambda = \mathrm{diag}(\lambda_{1}, \lambda_{2}, \ldots, \lambda_{n}) \tag{5}$$

When Φ_{C} contains all the element constant strains modes, the element formulation satisfies the patch test requirements necessary for solution convergence.

Further requirements regarding the entries of stiffness and mass matrices can be defined using geometrical symmetries of the element. If the element has some geometric symmetrical properties, then the mass and stiffness models reflect these properties; rotation of the element about its symmetry axes, e.g. x axis, by 180°, does not change the mass and stiffness matrices, that is

$$\mathbf{T}_{xx}^{T} \mathbf{K} \mathbf{T}_{xx} = \mathbf{K}, \quad \mathbf{T}_{xx}^{T} \mathbf{M} \mathbf{T}_{xx} = \mathbf{M} \tag{6}$$

where $\mathbf{T}_{xx}$ is a transformation matrix that rotates the element model about axis x by 180°.

It is possible to define a family of stiffness matrix for an element that satisfies the requirements mentioned in this section but depends upon one or more parameters. These parameters are identified by minimizing the element model discretization errors [9–14].

3 SHAPE FUNCTIONS ASSOCIATED WITH THE INVERSE MODELS

Hierarchal polynomials are employed to obtain shape functions of element models developed using an inverse approach. Hierarchal polynomial sets are defined using integrated Legendre polynomials. Zhu [19] initially presented the polynomial set and Bardell [16, 20] used the set to predict natural flexural vibrations of rectangular plates and skew plates. Zhu [19] introduced the polynomial set as

$$p_{m}^{s}(\zeta) = \sum_{n=0}^{m/2} \frac{(-1)^{n}}{2^{n} n!} \frac{(2m - 2n - 2s - 1)!!}{(m - 2n)!} \zeta^{m-2n} \tag{7}$$

where ζ is the element natural co-ordinate, $m!! = m(m - 2) \ldots (2$ or $1)$, $0!! = 1$, $(-1)!! = 1$, and $m/2$

Q3

denotes the integer part of this product [17]. The polynomial set (7) can be used as hierarchal shape functions with C^{s-1} continuity. Using Zhu's polynomials and considering the particular value $s = 2$, Bardell [16] proposed a hierarchal shape function of C^1 continuity. Hierarchal functions are constructed for two-dimensional (2D) or 3D elements by multiplications of two or three 1D functions defined in equations (7).

In general, the displacement field of an element is defined as

$$w(\zeta, \eta, \varsigma) = \sum_{i=1}^{N} N_i(\zeta, \eta, \varsigma) w_i \tag{8}$$

where $w(\zeta, \eta, \varsigma)$ is the displacement field, ζ, η, and ς are the element natural co-ordinates, $N_i(\zeta, \eta, \varsigma)$ is the ith shape function, w_i is nodal displacement, and N is the element number of DOF. The shape function $N_i(\zeta, \eta, \varsigma)$ is considered to be composed of two sets; the first set, $f_i(\xi, \eta, \varsigma)$, adopted from the classical FE model satisfying the element boundary conditions and the second set is defined using equation (7)

$$N_i(\xi, \eta, \varsigma) = f_i(\xi, \eta, \varsigma) + \sum_{m=1}^{n} a_m p_m^s(\zeta, \eta, \varsigma) \tag{9}$$

The unknown coefficients a_m and number of terms in polynomial series, n, are assigned to produce known stiffness and mass coefficients

$$k_{ij} = \int_0^1 \int_0^1 \int_0^1 \Gamma(N_i(\xi, \eta, \varsigma)) E(\xi, \eta, \varsigma)$$
$$\times \Gamma(N_j(\xi, \eta, \varsigma)) d\xi \, d\eta \, d\varsigma$$
$$m_{ij} = \int_0^1 \int_0^1 \int_0^1 N_i(\xi, \eta, \varsigma) \rho(\xi, \eta, \varsigma) N_j(\xi, \eta, \varsigma) d\xi \, d\eta \, d\varsigma \tag{10}$$

The operator Γ defines the strain field of the element, $E(\xi, \eta, \varsigma)$ is the elastic constant function and $\rho(\xi, \eta, \varsigma)$ specifies its mass density distribution. The process of satisfying these identities and obtaining the coefficients a_m is demonstrated in the next section for a membrane element in lateral vibrations.

4 FOUR-NODE RECTANGULAR TRANSVERSE MEMBRANE ELEMENT

Transverse membrane elements are a type of elements that only have out-of-plane degrees of freedom. These elements are used widely in the analysis of acoustic fields. The transverse membrane element reported in the literature is developed based on linear displacement assumption [21]. The resultant stiffness matrix presents a second-order convergence rate for static deflection problems both in local and in global systems. A more accurate transverse membrane stiffness model is obtained in this section via an
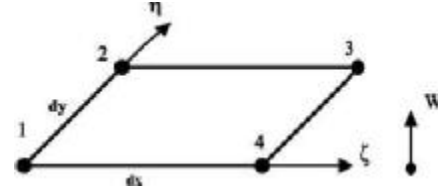

Fig. 1 Four-node square membrane element

inverse approach. Shape functions associated with the developed stiffness model are then determined using hierarchical polynomial sets.

4.1 Generic membrane element

A four-node rectangular membrane element with dimensions of Δx and Δy, shown in Fig. 1, is considered. Each node has one degree of freedom and the element stiffness matrix is a 4×4 symmetric positive semidefinite matrix of the following general form

$$\mathbf{K} = \kappa \begin{bmatrix} k_{11} & k_{12} & k_{13} & k_{14} \\ & k_{22} & k_{23} & k_{24} \\ & & k_{33} & k_{34} \\ \text{sym} & & & k_{44} \end{bmatrix} \tag{11}$$

where κ is a positive real scalar. A procedure similar to the one reported in reference [10] for a plate element is followed here to obtain the generic stiffness model of the membrane element.

The element has two symmetry axes; when the element is rotated 180° about one of these axes, the stiffness matrix remains unchanged. The rotations are equivalent to applying the transformations $\mathbf{T}_{xx}$ and $\mathbf{T}_{yy}$ as

$$\mathbf{T}_{xx}^{\mathrm{T}} \mathbf{K} \mathbf{T}_{xx} = \mathbf{K}, \quad \mathbf{T}_{yy}^{\mathrm{T}} \mathbf{K} \mathbf{T}_{yy} = \mathbf{K}, \quad \mathbf{T}_{xx} = \begin{bmatrix} 0 & 1 & 0 & 0 \\ 1 & 0 & 0 & 0 \\ 0 & 0 & 0 & 1 \\ 0 & 0 & 1 & 0 \end{bmatrix},$$

$$\mathbf{T}_{yy} = \begin{bmatrix} 0 & 0 & 0 & -1 \\ 0 & 0 & -1 & 0 \\ 0 & -1 & 0 & 0 \\ -1 & 0 & 0 & 0 \end{bmatrix} \tag{12}$$

Using the physical symmetry requirements, the number of unknown parameters of the stiffness matrix reduces to four

$$\mathbf{K} = \kappa \begin{bmatrix} k_{11} & k_{12} & k_{13} & k_{14} \\ & k_{11} & k_{14} & k_{13} \\ & & k_{11} & k_{12} \\ \text{sym} & & & k_{11} \end{bmatrix} \tag{13}$$

When the element is rotated through $\pi/2$ radians in its own plane, the element aspect ratio $q = \Delta x / \Delta y$ is

reversed. This rotation is equivalent to the transformation of

$$\mathbf{T}_{zz} = \begin{bmatrix} 0 & 0 & 0 & 1 \\ 1 & 0 & 0 & 0 \\ 0 & 1 & 0 & 0 \\ 0 & 0 & 1 & 0 \end{bmatrix}, \quad \mathbf{T}_{zz}^{\mathrm{T}} \cdot \mathbf{K}(q) \cdot \mathbf{T}_{zz} = \mathbf{K}(1/q) \quad (14)$$

It leads directly from equation (14) that k_{14} is obtained by inverting the aspect ratio q to $1/q$ in k_{12}; this produces one more constraint on the parameters of the element.

The element has one rigid-body mode

$$\phi_{\mathrm{R}} = [1\ 1\ 1\ 1]^{\mathrm{T}} \tag{15}$$

Introducing the rigid-body mode into equation (1), one more parameter is defined as

$$\mathbf{K}\phi_{\mathrm{R}} = 0 \Rightarrow k_{13} = -(k_{11} + k_{12} + k_{14}) \tag{16}$$

This brings the total number of un-attributed parameters of the parametric stiffness matrix to three. The element has two constant strain modes

$$\phi_{\mathrm{c1}} = \begin{bmatrix} -\dfrac{1}{2} & \dfrac{1}{2} & \dfrac{1}{2} & -\dfrac{1}{2} \end{bmatrix}^{\mathrm{T}}, \quad \phi_{\mathrm{c2}} = \begin{bmatrix} -\dfrac{1}{2} & -\dfrac{1}{2} & \dfrac{1}{2} & \dfrac{1}{2} \end{bmatrix}^{\mathrm{T}} \tag{17}$$

These constant strain modes produce the following strain energies in the element

$$\lambda_1 = \frac{P}{q}, \quad \lambda_2 = Pq \tag{18}$$

where P is the surface tension at the edges of element. Employing the constant strain relations defined in equation (3), one finds the following requirements on the element entries

$$k_{12} = \frac{P}{2\kappa}q - k_{11}, \quad k_{14} = \frac{P}{2\kappa q} - k_{11} \tag{19}$$

There remains only one unknown parameter in the stiffness matrix determined by minimizing the discretization errors in the element formulations.

4.2 Discretization error analysis

The formulation obtained from the parametric stiffness matrix is compared with the governing equation of the transverse membrane, allowing identification of the un-attributed parameters by minimizing the discretization errors.

The membrane elements with an area $\Delta A = \Delta x \times \Delta y$ are assembled to create finite-element model of a rectangular membrane with free edges, as shown in
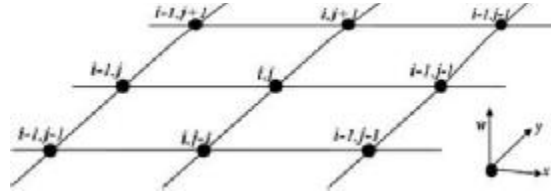

Fig. 2 Assembled square membrane elements

Fig. 2. In the assembled model, the discrete equation of motion corresponding to a typical internal node (i, j) is

$$\kappa[\alpha, \ \beta, \ \alpha, \ \beta, \ 4k_{11} \ \beta, \ \alpha, \ \beta, \ \alpha] \begin{Bmatrix} \vdots \\ d_{i,j-1} \\ d_{i,j} \\ d_{i,j+1} \\ \vdots \end{Bmatrix},$$

$$\alpha = k_{11} - \frac{P}{\kappa}, \quad \beta = \frac{P}{\kappa} - 2k_{11} \tag{20}$$

This discrete governing equation is then converted to a continuous series form by defining the deformations in the neighbouring nodes using Taylor series expansions of deformations in node (i, j)

$$d_{i\pm1,j\pm1} = d_{i,j} + \sum_{n=1}^{\infty} \frac{1}{n!} \left(\pm\Delta x \frac{\partial}{\partial x} \pm \Delta y \frac{\partial}{\partial y} \right)^n d_{i,j} \tag{21}$$

This process transforms the discrete finite-element equations into a partial differential equation in series form having the terms of an increasing order of smallness $O(\Delta x^{2n}, \Delta y^{2n})$, $n = 1, 2, \ldots$. The continuous form can be written as

$$\begin{aligned}
&\Delta A P \left(\frac{\partial^2 w}{\partial x^2} + \frac{\partial^2 w}{\partial y^2} \right) \\
&+ \sum_{n=1}^{\infty} \Delta A^{n+1} \left[\frac{P}{q^{n-1}} \frac{\partial^2 n}{\partial^2 n} \left(\frac{1}{q(n+1)(2n+1)!} \frac{\partial^2 w}{\partial x^2} \right. \right. \\
&\left. + \frac{1}{6^{n-1}} \left(\frac{1}{4q} + \frac{q}{4} - \frac{\kappa k_{11}}{2P} \right) \frac{\partial^2 w}{\partial y^2} \right) \\
&+ Pq^{n-1} \frac{\partial^{2n}}{\partial y^{2n}} \left(\frac{1}{q(n+1)(2n+1)!} \frac{\partial^2 w}{\partial y^2} \right. \\
&\left. \left. + \frac{1}{6^{n-1}} \left(\frac{1}{4q} + \frac{q}{4} - \frac{\kappa k_{11}}{2P} \right) \frac{\partial^2 w}{\partial x^2} \right) \right]
\end{aligned} \tag{22}$$

The resultant continuous differential equations must produce the left-hand side of transverse membrane motion governing the equation

$$P \left(\frac{\partial^2 w}{\partial x^2} + \frac{\partial^2 w}{\partial y^2} \right) = -F(x, y) \tag{23}$$

where $F(x, y)$ is the distributed lateral external force. The characteristic area ΔA is an independent variable;

therefore, to compare the obtained series equation with the exact equation of motion one may start from the lowest-order terms and assign the stiffness parameters to minimize the difference between the two models. The lowest-order term in equation (22) is of order ΔA and is equal to the left-hand side of equation of motion (23). Next, the terms of order ΔA^2 are considered

$$\Delta A^2 P \left[\frac{\partial^2}{\partial x^2} \left(\frac{1}{12q} \frac{\partial^2 w}{\partial x^2} + \left(\frac{1}{4q} + \frac{q}{4} - \frac{\kappa k_{11}}{2P} \right) \frac{\partial^2 w}{\partial y^2} \right) \right.$$
$$\left. + \frac{\partial^2}{\partial y^2} \left(\frac{q}{12} \frac{\partial^2 w}{\partial y^2} + \left(\frac{1}{4q} + \frac{q}{4} - \frac{\kappa k_{11}}{2P} \right) \frac{\partial^2 w}{\partial x^2} \right) \right] \tag{24}$$

Equation (24) represents the left-hand side of the equation of motion when the following three requirements are met

$$\kappa = P \tag{25}$$

$$\left(\frac{1}{q} + q - 2k_{11} \right) = \frac{1}{3q} \tag{26}$$

$$\left(\frac{1}{q} + q - 2k_{11} \right) = \frac{q}{3} \tag{27}$$

Obviously, the requirements of equations (26) and (27) cannot be satisfied simultaneously when $q \neq 1$. Therefore, one may look for a least square solution by assigning

$$k_{11} = \frac{5}{12} \left(q + \frac{1}{q} \right) \tag{28}$$

This results in the SCS matrix of the transverse membrane element as

$$\mathbf{K} = \frac{P}{12q} \begin{bmatrix} 5(q^2 + 1) & 1 - 5q^2 & -(q^2 + 1) & q^2 - 5 \\ & 5(q^2 + 1) & q^2 - 5 & -(q^2 + 1) \\ & & 5(q^2 + 1) & 1 - 5q^2 \\ \text{sym} & & & 5(q^2 + 1) \end{bmatrix},$$
$$q = \frac{\Delta x}{\Delta y} \tag{29}$$

When the aspect ratio of elements are set to unity ($q = 1$), the residues of equations (26) and (27) are zero and the discretization errors are of sixth order (i.e. $O(\Delta x^6)$). The element developed using linear shape functions with $k_{11} = 1/3[q + (1/q)]$ produces errors of $O(\Delta x^4)$.

The stiffness matrix of equation (29) is developed in the local co-ordinates. It is desired to obtain the associate shape functions for the new optimum stiffness matrix to be able to transform it to global co-ordinates.

4.3 Shape functions of the SCS model

The displacement field of the membrane element is defined as

$$w(\zeta, \eta) = N_1(\zeta, \eta)w_1 + N_2(\zeta, \eta)w_2$$
$$+ N_3(\zeta, \eta)w_3 + N_4(\zeta, \eta)w_4 \tag{30}$$

where ζ and η are natural co-ordinates of the element $\zeta = x/dx, \eta = y/dy$, as shown in Fig. 1. The element has one rigid-body mode of $\phi_{R1} = [1, 1, 1, 1]$, which enforces the following requirement on the shape functions of the membrane element

$$N_1(\zeta, \eta) + N_2(\zeta, \eta) + N_3(\zeta, \eta) + N_4(\zeta, \eta) = 1 \tag{31}$$

Requirement (31) relates $N_4(\zeta, \eta)$ to other shape functions expressed as a linear combination of the hierarchal functions. Following Bardell [16], the membrane element shape functions are formed from two sets of polynomials

$$N_1(\xi, \eta) = f_1(\xi, \eta) + \sum_{i=1}^{N} a_{i+2} f_{i+2}(\zeta, \eta)$$

$$N_2(\xi, \eta) = f_1(\xi, 1 - \eta) + \sum_{i=1}^{N} a_{i+2} f_{i+2}(\zeta, 1 - \eta)$$

$$N_3(\xi, \eta) = f_1(1 - \xi, 1 - \eta) + \sum_{i=1}^{N} a_{i+2} f_{i+2}(1 - \zeta, 1 - \eta) \tag{32}$$

The first part is adopted from the classical membrane element model shape functions to satisfy the element boundary conditions. The complementary parts of shape functions are defined using hierarchal functions. These 2D polynomial functions are constructed by multiplications of two 1D polynomial functions, that is

$$f_r(\zeta, \eta) = f_r(\zeta) f_r(\eta) \tag{33}$$

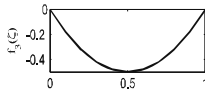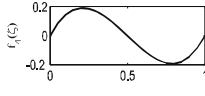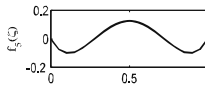The base polynomial satisfying membrane element boundary conditions is

$$f_1(\zeta) = 1 - \zeta \tag{34}$$

and the complementary parts are defined using equation (7) as

$$f_r(\zeta) \equiv P^{s=1}_{m=r-1}(\zeta)$$
$$= \sum_{n=0}^{(r-1)/2} \frac{(-1)^n}{2^n n!} \frac{(2r - 2n - 5)!!}{(r - 2n - 1)!} \zeta^{r-2n-1}, \quad r > 2 \tag{35}$$

Shape functions of the membrane element have C^0 continuity; thus, s in $p^s_m(\zeta)$ is set to unity. Table 1

Table 1 Hierarchal polynomials obtained using equation (31)

$f_3(\xi) = 2\xi^2 - 2\xi$

$f_4(\xi) = 4\xi^3 - 6\xi^2 + 2\xi$

$f_5(\xi) = 10\xi^4 - 20\xi^3 + 12\xi^2 - 2\xi$

demonstrates these functions $(2 < r < 5)$, and it can be seen that the polynomial sets have zero displacements at element nodes, while their slopes are non-zero at these locations.

Q5 The element has two symmetry axes and an applied displacement at one node whereas other nodes are fixed, apart from a constant, and produces an anti-symmetric deformation $w(\zeta, \eta)$ with respect to the element's natural co-ordinates. The selected form for the shape functions in equations (32) to (35) reflects this fact. Changing the unit displacement practice from one node to the neighbouring one, the deformation field of the element is rotated by $\pi/2$ about axes normal to the element plane. This property is also represented in the functions introduced in equations (32) to (35). There is one more requirement that must be satisfied by series defined in equation (32) leading to the specifications of series coefficients a_i. These functions must produce the entries of membrane SCS defined in equation (29), that is

$$k_{ij} = P \int_0^1 \int_0^1 ab \left(\frac{1}{a^2} \frac{\partial N_i}{\partial \xi} \frac{\partial N_j}{\partial \xi} + \frac{1}{b^2} \frac{\partial N_i}{\partial \eta} \frac{\partial N_j}{\partial \eta} \right) d\xi \, d\eta \tag{36}$$

The requirement defined in equation (36) produces one independent equation to be satisfied. The hierarchal polynomials of equation (32) must contain only odd functions to produce the required anti-symmetric deflection; therefore, a_3 is set to zero and a_4 is obtained by satisfying equation (36) as

$$a_4 = \frac{5}{8}\sqrt{14} \tag{37}$$

The obtained hierarchal shape function $N_1(\zeta, \eta)$ of the rectangular membrane SCS is shown in Fig. 3. The other three shape functions are obtained by rotation of $N_1(\zeta, \eta)$ about the axis normal to the element plane. The numerical performance of the transverse membrane element is evaluated in the global co-ordinates using these new shape functions and its
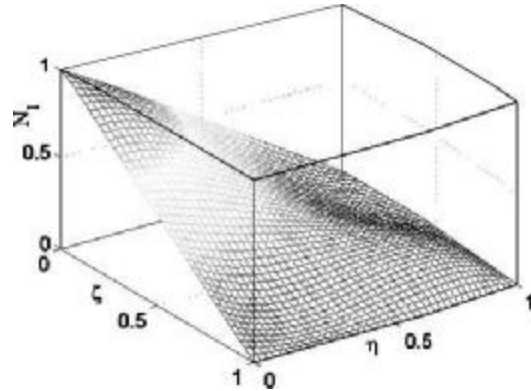
Fig. 3 Shape function $N_1(\xi, \eta)$ of transverse membrane element

convergence rate in estimating the membrane deflection are demonstrated in the next section.

5 NUMERICAL STUDY

In the following numerical examples, errors in estimation of mid-node deflection due to the uniform pressure of clamped square and sectorial membranes are investigated. Exact analytical solutions of square and sectorial membrane deformations under uniform pressure are available. These solutions are compared with the numerical finite-element results to estimate the discretization errors. The results are obtained in non-dimensional form and are independent of the size of membranes. This allows comparing discretization errors of the classical and inverse membrane models.

The clamped square membrane subjected to uniformly distributed load is modelled using two different formulations, namely the stiffness model obtained from bi-linear shape functions and the stiffness matrix developed using the inverse approach. Figure 4 shows error in the estimation of the static deflection of the membrane's centre node and the convergence rate of these models when the number of elements $(q = 1)$ are increased. As shown in Fig. 4, the convergence rate in the bi-linear model is of second order whereas the order of error in the model formed using the proposed stiffness matrix is of fourth order. This example demonstrates the superiority of the obtained model using the inverse approach over the existing one.

In a second example, the deformation of a clamped sectorial membrane with radius ratio of 2 and centre angle of $90°$, as shown in Fig. 5, subjected to uniformly distributed pressure is considered. The membrane is modelled using the stiffness models obtained from bi-linear shape functions and the inverse approach. Then the elements are transformed from the local rectangular shape to the global quadrilateral form, as shown in Fig. 6, to model the sectorial membrane. Figure 7 shows the error in estimation of sectorial
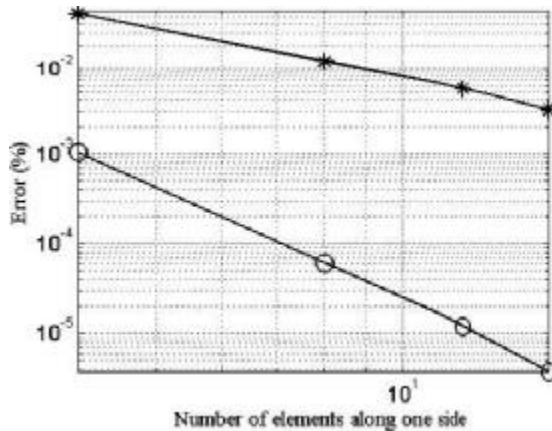
Fig. 4 Errors in estimating mid-node deflection of a square membrane (proposed model – circles and bi-linear shape function – stars)
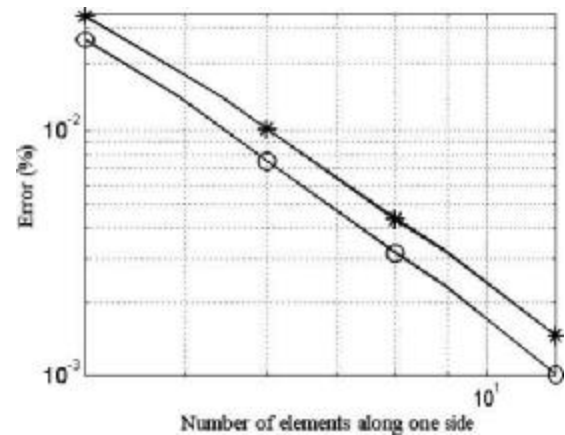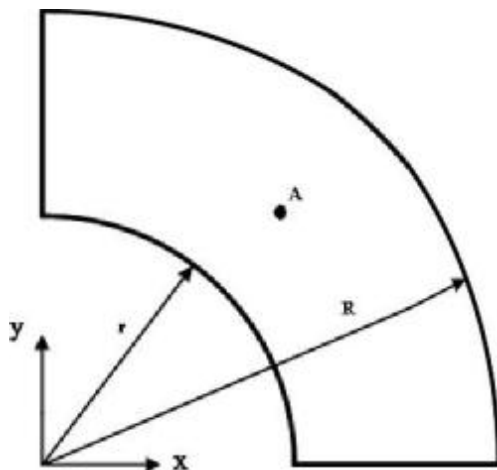

Fig. 5 Open sectorial membrane, dimension ($R/r = 2$) (m)

Q6

Fig. 6 Two-dimensional 'mapping' of square element

membrane centre node static deflection. The centre node is designated as point A in Fig. 5 and has co-ordinates of $r = 0.75$, $\theta = 45°$. The convergence rates of both classical and inverse models are investigated by increasing the mesh numbers. In this numerical study, the number of elements in radial and tangential

Fig. 7 Errors in estimating mid-node deflection of a sector membrane (proposed model – circles and bi-linear shape function – stars)

directions is kept the same whereas the number of meshes along each side is increased from 4 to 12. As shown in Fig. 7, the inverse model creates more accurate results. The convergence rate in both models is of second order due to the fact that the aspect ratio of the element is not unity; therefore, the discretization errors in both models are of fourth order.

The order of the element model obtained from the proposed method of the present article is equal to the one obtained from bi-linear shape functions while the accuracy of the inverse model is superior to the bi-linear model. This leads to equal computational efforts to solve a problem using either element models, but the proposed model creates more accurate results at no added computational costs.

6 CONCLUSION

A procedure is developed in this article to generate the shape functions associated with the super-convergent element formulations. The shape functions are formed using the classical shape functions of the element, satisfying its boundary conditions, and hierarchal polynomial sets. The coefficients of the polynomials are assigned such that the optimum formulation for the element in terms of its accuracy is achieved in local co-ordinates. The proposed procedure is demonstrated for a transverse membrane element. First, the super-convergent element formulation is obtained using an inverse approach. Next, the element shape functions are obtained using hierarchal polynomial sets and its displacement field is transformed to the global co-ordinates using these shape functions. Numerical examples employed to demonstrate more accurate results are obtained using the new formulation at no added computational costs.

REFERENCES

1 **Houmat, A.** A sector elliptic p-element applied to membrane vibrations. *Thin-Walled Struct.*, 2009, **47**, 172–177.
2 **Houmat, A.** Free vibration analysis of arbitrarily shaped membranes using the trigonometric p-version of the finite element method. *Thin-Walled Struct.*, 2006, **44**, 943–951.
3 **Houmat, A.** A sector Fourier p-element for free vibration analysis of sectorial membranes. *Comput. Struct.*, 2001, **79**, 1147–1152.
4 **Leung, A.** and **Chan, J.** Fourier p-element for the analysis of beam and plates. *J. Sound Vibr.*, 1998, **212**, 79–85.
5 **Bert, C.** and **Malik, M.** The differential quadrature method for irregular domains and application to plate vibration. *Int. J. Mech. Sci.*, 1996, **38**, 589–606.
6 **Wang, X., Bert, C.,** and **Striz, A.** A new approach in applying differential quadrature and free vibrational analysis of beams and plates. *J. Sound Vibr.*, 1993, **162**, 566–572.
7 **Xing, Y.** and **Liu, B.** High accuracy differential quadrature finite element method and its application to free vibrations of thin plate with curvilinear domain. *Int. J. Numer. Meth.*, 2009, **80**, 1718–1742.
8 **Wanji, C.** and **Cheung, Y. K.** Refined non-conforming quadrilateral thin plate bending element. *Int. J. Numer. Meth.*, 1997, **40**, 3919–3935.
9 **Stavrinidis, C., Clinckemaillie, J.,** and **Dubois, J.** New concepts for finite element mass matrix formulation. *J. AIAA*, 1989, **27**, 1249–1255.
10 **Ahmadian, H., Friswell, M. I.,** and **Mottershead, J. E.** Minimization of the discretization error in mass and stiffness formulation by inverse method. *Int. J. Numer. Meth. Engng*, 1998, **41**, 371–387.
11 **Kim, K.** A review of mass matrices for eigenproblems. *Comput. Struct.*, 1993, **46**, 1041–1048.
12 **Hansson, P. A.** and **Goransandberg.** Mass matrices by minimization of modal errors. *Int. J. Numer. Meth. Engng*, 1997, **40**, 4259–4271.
13 **Fried, I.** and **Chavez, M.** Superaccurate finite element eigenvalue computation. *J. Sound Vibr.*, 2004, **275**, 415–422.
14 **Fried, I.** and **Leong, K.** Super accurate finite element eigenvalue via a Rayleigh quotient correction. *J. Sound Vibr.*, 2005, **288**, 375–386.
15 **Houmat, A.** Hierarchical finite element analysis of the vibration of membranes. *J. Sound Vibr.*, 1997, **201**, 465–472.
16 **Bardell, N. S.** Free vibration analysis of flat plate using the hierarchical finite element method. *J. Sound Vibr.*, 1991, **151**, 263–289.
17 **Beslin, O.** and **Nicolas, J.** A hierarchical function set for predicting very high order plate bending modes with any boundary conditions. *J. Sound Vibr.*, 1997, **202**, 633–655.
18 **Taazount, M., Zinai, A.,** and **Bouazzouni, A.** Large free vibration of thin plates: hierarchic finite element method and asymptotic linearization. *Euro. J. Mech. A Solids*, 2009, **28**, 155–165.
19 **Zhu, D. C.** Development of hierarchal finite element methods at BIAA. In Proceedings of the International Conference on *Computational mechanics*, Tokyo, 1986.
20 **Bardell, N. S.** The free vibration of skew plates using the hierarchal finite element method. *Comput. Struct.*, 1992, **45**, 841–874.
21 **Kwon, Y.** and **Bang, H.** *The finite element method using Matlab*, 2nd edition, 2000 (CRC press, Boca Raton, Florida).

APPENDIX

NOTATION

a_m	coefficient of hierarchal polynomial sets
$d_{i,j}$	node displacement
$E(\xi, \eta, \varsigma)$	elastic constant function
$f_i(\xi, \eta, \varsigma)$	classical finite-element shape functions
$I_{xx}, I_{yy},$ and I_{zz}	moments of inertia
$\mathbf{K}$	stiffness matrix
m	element mass
$\mathbf{M}$	mass matrix
N	Number of DOF
$N_i(\zeta, \eta, \varsigma)$	shape functions
$p_m^s(\zeta, \eta, \varsigma)$	hierarchal polynomial sets
P	surface tension
q	aspect ratio of the element
$\mathbf{T}_{xx}$	transformation matrix about axis x
$\mathbf{T}_{yy}$	transformation matrix about axis y
$w(\zeta, \eta, \varsigma)$	displacement of element
w_i	nodal lateral displacement
Γ	strain field of the element
ΔA	element area
Δx	element length
Δy	element width
ε_i	strain vector
ζ, η and ς	element natural co-ordinates
κ	real positive scalar
λ_i	strain energy stored in the element at the ith constant strain mode
Λ	diagonal matrix with entries λ_i
$\rho(\xi, \eta, \varsigma)$	mass density
σ_i	stress vector
Φ_C	matrix of constant strain modes
Φ_R	matrix of rigid-body modes of element

JMES2350

Q1 Please confirm if in the sentence "There are different approaches to improve...", **change from "differentate equation" to "differential equation" OK.**

Q2 Please confirm if change from "Hanssan [12]" to "Hansson [12]" OK.

Q3 As per our style, vectors are bold italic and matrices bold upright. Please check we have correctly identified **all occurrences.**

Q4 Please expand "DOF".

Q5 Please confirm if changes made in the sentence "The element has two symmetry axes ..." **OK.**

Q6 Please confirm if caption for Fig. 5 OK as edited.

Q7 Please provide initial of 2nd author in Ref. [12].

Q8 In Ref. [19], please confirm expansion of proceeding title OK.